Syntheses and Crystal Structures of the Bromide-derivatized Lanthanoid(III) Ortho-Oxomolybdates(VI) *Ln*Br[MoO_4] (*Ln* = Pr, Nd, Sm, Gd – Lu)

Tanja Schustereit, Harald Henning, Thomas Schleid, and Ingo Hartenbach

University of Stuttgart, Institute for Inorganic Chemistry, Pfaffenwaldring 55, D-70569 Stuttgart, Germany

Reprint requests to Dr. Ingo Hartenbach. Fax: +49-711-685-54254.
E-mail: hartenbach@iac.uni-stuttgart.de

Z. Naturforsch. **2013**, *68b*, 616 – 624 / DOI: 10.5560/ZNB.2013-3083
Received February 20, 2013

Dedicated to Professor Heinrich Nöth on the occasion of his 85th birthday

The lanthanoid(III) bromide ortho-oxomolybdates(VI) *Ln*Br[MoO_4] (*Ln* = Pr, Nd, Sm, Gd – Lu) crystallize triclinically in the space group $P\bar{1}$ ($a = 686 - 689$, $b = 713 - 741$, $c = 1066 - 1121$ pm, $\alpha = 103 - 106$, $\beta = 107 - 108$, $\gamma = 92 - 95°$) with $Z = 4$. The crystal structure contains two crystallographically distinguishable Ln^{3+} cations, each one with a coordination number of seven *plus* one. $(Ln1)^{3+}$ is surrounded by three bromide and four *plus* one oxide anions, while for $(Ln2)^{3+}$ just one bromide and six *plus* one oxide anions belong to the coordination sphere. Considering the smallest lanthanoids, however, the distances to the farthest anions increase so much that their contribution to the coordination spheres becomes negligible in both cases. The polyhedra around $(Ln1)^{3+}$ are connected to each other *via* common edges, which consist of two crystallographically identical Br^- anions (Br1). Furthermore, the common structure of the *Ln*Br[MoO_4] series contains two crystallographically different, discrete $[MoO_4]^{2-}$ ortho-oxomolybdate(VI) tetrahedra. Two *plus* one oxygen atoms of each $[(Mo1)O_4]^{2-}$ unit are used to interconnect the polyhedra around $(Ln1)^{3+}$ and $(Ln2)^{3+}$ together with one Br^- anion (Br2). The connection between two polyhedra around $(Ln2)^{3+}$ is generated exclusively by two *plus* one oxygen atoms of two $[(Mo2)O_4]^{2-}$ anions. The complete structural arrangement can be considered as a bundle of primitively packed $^1_\infty\{Ln\mathrm{Br}[MoO_4]\}$ chains with two alternating motifs of linkage, which are running parallel along [012].

Key words: Lanthanoids, Bromides, Oxomolybdates, Crystal Structure

Introduction

In the last few years, the number of crystal structures of rare earth metal(III) halide oxomolybdates(VI) with the formula *REX*[MoO_4] (*RE* = Y, La – Nd, Sm – Lu; *X* = F, Cl, Br) known to literature increased tremendously, owing to their potential as host lattices for luminescent Ln^{3+} dopants of the lanthanoid series (*Ln* = Ce – Yb). All of them show a structural gap between the lighter and the heavier lanthanides (*plus* yttrium). The rare earth metal(III) fluoride oxomolybdates(VI) with the formula *RE*F[MoO_4] are only known for yttrium and the heavier cations (*RE* = Y [1], Sm – Tm [2]) so far, while for the lighter lanthanide elements only the fluoride-poor compound $La_3F[MoO_4]_4$ [3] has been structurally characterized. Its structure comprises the halide anion surrounded by three La^{3+} cations and besides, three crystallographically independent, but isolated $[MoO_4]^{2-}$ tetrahedra, and another one with a coordination number of four *plus* one is observed as a trigonal-bipyramidal $[MoO_{4+1}]^{4-}$ unit. Similar $[MoO_5]^{4-}$ polyhedra are also found in the rare earth metal(III) chloride oxomolybdates(VI) with the formula *Ln*Cl[MoO_4] (*Ln* = La – Pr) [4] as well as their bromide homologs *Ln*Br[MoO_4] (*Ln* = La and Ce) [5]. While in $La_3F[MoO_4]_4$ [3] the halide anion is coordinated by only three La^{3+} cations, this coordination number increases to three *plus* one in the aforementioned compounds *REX*[MoO_4] comprising only the largest rare earth metals. Furthermore, in all these structures the coordination spheres of the RE^{3+} cations

consist of nine or even nine *plus* one oxide and halide anions, and are thus considerably larger than those with coordination numbers of seven or eight as found in the halide derivatives with the formula $REX[MoO_4]$ with yttrium and the heavier lanthanoid cations (RE = Y, Nd, Sm – Lu). The crystal structures of the REF[MoO_4] (RE = Y [1], Sm – Tm [2]) and the RECl[MoO_4] series (RE = Y [1], Sm – Yb [6]) both display six oxide and two halide anions in the coordination spheres of the RE^{3+} cations, while in LuCl[MoO_4] [6] this environment is even reduced by one O^{2-} anion to a coordination number of only seven. Two common features of all structures with the smaller rare earth metal(III) cations are the angular RE^{3+} coordination at the X^- anions for CN = 2 and the exclusive presence of isolated $[MoO_4]^{2-}$ tetrahedra. In the crystal structure of the title compounds with the formula LnBr[MoO_4], these common characteristics persist, however, the coordination environment around the Ln^{3+} cations (Ln = Pr, Nd, Sm, Gd – Lu) differs significantly from that of the light-halide derivatives ($REX[MoO_4]$ with X = F and Cl).

Experimental Section

Syntheses of the members of the LnBr[MoO4] series (Ln = Pr, Nd, Sm, Gd – Lu)

The lanthanoid(III) bromide ortho-oxomolybdate(VI) representatives were obtained by solid-state reactions of mixtures of the respective lanthanoid tribromides ($PrBr_3$, $NdBr_3$, $SmBr_3$, $GdBr_3$, $TbBr_3$, $DyBr_3$, $HoBr_3$, $ErBr_3$, $TmBr_3$, $YbBr_3$, $LuBr_3$: all 99.9 %; Aldrich, Taufkirchen, Germany), the corresponding lanthanoid sesquioxides (Nd_2O_3, Lu_2O_3: both 99.9 %, Heraeus, Hanau, Germany; Sm_2O_3, Gd_2O_3, Dy_2O_3, Ho_2O_3, Er_2O_3, Tm_2O_3, Yb_2O_3: all 99.9 %; ChemPur, Karlsruhe, Germany) and molybdenum trioxide (MoO_3: p. a.; Merck, Darmstadt, Germany) with $LnBr_3$: Ln_2O_3 : MoO_3 in molar ratios of 1 : 1 : 3 in evacuated silica ampoules heated for seven days at 820 °C according to Eq. 1.

$$LnBr_3 + Ln_2O_3 + 3\,MoO_3 \rightarrow 3\,LnBr[MoO_4] \quad (1)$$

Since Pr_2O_3 and Tb_2O_3 were not available from commercial sources, these oxides had to be produced *in situ* by synproportionation of the elemental lanthanoid (Pr, Tb: both 99.9 %; ChemPur, Karlsruhe, Germany) and the appropriate amount of lanthanoid(III,IV) oxide (Pr_6O_{11}, Tb_4O_7: both 99.9 %; ChemPur, Karlsruhe, Germany) according to the Eqs. 2 and 3 in order to finally obtain the LnBr[MoO_4] representatives with Ln = Pr and Tb.

$$4\,Pr + 3\,Pr_6O_{11} \rightarrow 11\,Pr_2O_3 \quad (2)$$

$$2\,Tb + 3\,Tb_4O_7 \rightarrow 7\,Tb_2O_3 \quad (3)$$

In all reactions, coarse and transparent single crystals emerged, which remained stable in air and water and showed the color of the respective lanthanoid trication (colorless for Ln = Gd – Dy, Tm – Lu; green for Ln = Pr; lilac for Ln = Nd; yellow for Ln = Sm and Ho; pink for Ln = Er). Due to redox processes between the bromide anions and hexavalent molybdenum, the title compounds do not occur as pure phases, but with a variety of by-products consisting mostly of reduced molybdenum oxides such as MoO_2. Furthermore, gaseous Br_2 was identified in the afore evacuated silica ampoules after the reaction. It was not possible to obtain the europium representative with this preparative method, owing to the reductive action of bromide anions on Eu^{3+} due the special stability of divalent europium.

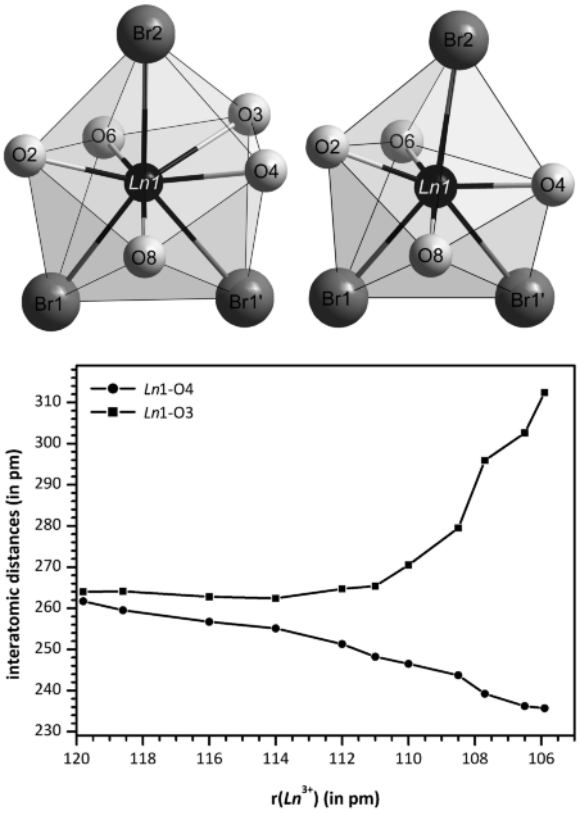

Fig. 1. Coordination polyhedra around the $(Ln1)^{3+}$ cations (Ln = Pr, Nd, Sm, Gd – Er, top left; Ln = Tm – Lu, top right) and a graphical display of the second longest (Ln1–O3) and longest Ln–O distances (Ln1–O4) in the crystal structure of the LnBr[MoO_4] representatives with Ln = Pr, Nd, Sm and Gd – Lu (bottom).

Table 1. Crystal structure data for LnBr[MoO_4] (Ln = Pr, Nd, Sm, Gd – Lu).

	PrBr[MoO_4]	NdBr[MoO_4]	SmBr[MoO_4]	GdBr[MoO_4]	TbBr[MoO_4]	DyBr[MoO_4]	HoBr[MoO_4]	ErBr[MoO_4]	TmBr[MoO_4]	YbBr[MoO_4]	LuBr[MoO_4]
Crystal system, formula units	triclinic, $Z = 4$										
Space group	$P\bar{1}$ (no. 2)										
Lattice parameters											
a, pm	697.95(2)	695.29(2)	691.38(2)	688.53(2)	686.64(2)	685.65(2)	685.16(2)	684.81(2)	686.10(2)	686.00(2)	685.94(2)
b, pm	740.69(2)	737.56(2)	730.78(2)	726.28(2)	722.06(2)	719.13(2)	717.93(2)	716.00(2)	715.04(2)	713.24(2)	712.70(2)
c, pm	1120.88(4)	1117.70(4)	1110.45(4)	1105.93(4)	1097.05(4)	1093.19(4)	1088.32(4)	1081.35(4)	1074.55(4)	1069.73(4)	1066.18(4)
α, deg	105.945(2)	106.061(2)	106.061(2)	106.142(2)	105.574(2)	105.397(2)	105.031(2)	104.430(2)	103.623(2)	103.234(2)	102.954(2)
β, deg	106.702(2)	106.743(2)	106.983(2)	107.098(2)	107.262(2)	107.332(2)	107.342(2)	107.455(2)	107.627(2)	107.665(2)	107.688(2)
γ, deg	92.355(2)	92.329(2)	92.239(2)	92.260(2)	92.526(2)	92.750(2)	93.145(2)	93.664(2)	94.238(2)	94.712(2)	95.034(2)
Calculated density, D_x, g·cm^{-3}	4.78	4.88	5.07	5.24	5.34	5.44	5.51	5.58	5.63	5.73	5.78
Molar volume, V_m, cm^3·mol^{-1}	79.658	78.728	76.968	75.776	74.646	73.971	73.534	72.912	72.606	72.107	71.826
F(000), e	672	676	684	692	696	700	704	708	712	716	720
Index range, $\pm h$ / $\pm k$ / $\pm l$	9 / 9 / 14	9 / 9 / 14	9 / 9 / 14	9 / 9 / 14	9 / 9 / 14	8 / 9 / 14	9 / 9 / 14	9 / 9 / 14	9 / 9 / 14	9 / 9 / 14	9 / 9 / 14
$2\theta_{max}$, deg	56.46	56.49	56.47	56.30	56.49	54.87	56.30	56.29	56.29	56.46	56.47
Absorption coefficient, μ, mm^{-1}	18.9	19.8	21.5	23.4	24.6	25.7	26.7	27.9	29.1	30.3	31.5
Data corrections	background, polarization, and Lorentz factors; numerical absorption correction with the program HABITUS [7]										
Reflections (collected / unique)	12975 / 2609	16516 / 2581	16980 / 2516	18881 / 2461	18011/ 2443	15262 / 2245	17998 / 2388	18102 / 2376	17638 / 2376	16840 / 2370	17520 / 2365
R_{int} / R_σ	0.082 / 0.045	0.098 / 0.051	0.121 / 0.058	0.088 / 0.046	0.082 / 0.034	0.101 / 0.049	0.074 / 0.036	0.055 / 0.024	0.093 / 0.049	0.095 / 0.040	0.101 / 0.045
Structure solution and refinement	program package SHELX-97 [8], scattering factors according to International Tables, Vol. C [9]										
R_1 for (n) reflections with $\lvert F_o \rvert > 4\ \sigma(F_o)$	0.028 (2328)	0.034 (2083)	0.032 (2027)	0.027 (1921)	0.021 (2290)	0.035 (1831)	0.023 (2002)	0.023 (2263)	0.034 (1877)	0.029 (2174)	0.027 (1976)
R_1 / wR_2 for all reflections	0.033 / 0.070	0.050 / 0.070	0.048 / 0.074	0.047/ 0.049	0.024 / 0.049	0.048 / 0.085	0.033 / 0.045	0.024 / 0.056	0.053 / 0.069	0.033 / 0.072	0.038 / 0.060
Goodness of Fit (GooF)	1.043	1.043	1.008	1.016	1.072	1.036	1.049	1.154	1.047	1.069	1.006
Extinction, g	0.0576(11)	0.0044(2)	0.0060(3)	0.00174(11)	0.0103(3)	0.0018(3)	0.060(2)	0.05001(8)	0.0049(2)	0.056(3)	0.027(2)
Residual electron density, ρ, e$^- \times 10^{-6}$ pm^{-3}, min. /max.	−1.66 / 2.22	−1.28 / 1.87	−1.63 / 2.10	−1.40 / 1.26	−1.59 / 1.65	−1.84 / 2.34	−1.16 / 1.06	−2.55 / 1.41	−1.65 / 1.88	−1.98 / 2.82	−1.80 / 1.60
CSD numbers	425263	425264	425265	425266	425267	425268	425269	425270	425271	425272	425273

Table 2. Interatomic distances (d in pm, esd = ±0.1) and selected bond angles (∠ in deg, esd = ±0.1) for the triclinic LnBr[MoO_4] series (Ln = Pr, Nd, Sm, Gd – Lu).

Ln	Pr	Nd	Sm	Gd	Tb	Dy	Ho	Er	Tm	Yb	Lu
*Ln*1–O6	238.4	237.8	233.9	231.6	229.5	227.6	228.0	226.0	224.8	222.9	222.5
*Ln*1–O8	239.0	238.8	234.2	232.9	231.0	229.0	228.4	227.9	224.9	224.0	223.1
*Ln*1–O2	241.4	238.0	238.4	234.7	233.3	232.7	231.2	228.7	223.6	224.5	222.9
*Ln*1–O4	261.7	259.5	256.7	255.1	251.3	248.2	246.5	243.7	239.2	236.2	235.7
*Ln*1–O3	264.0	264.1	262.8	262.4	264.7	265.4	270.5	279.5	*295.9*	*302.6*	*312.4*
*Ln*1–Br1	298.0	296.6	292.6	290.0	288.4	287.3	286.7	286.0	286.5	284.8	283.5
*Ln*1–Br1′	298.9	297.3	294.6	292.8	291.6	290.9	289.9	288.5	286.7	286.1	286.2
*Ln*1–Br2	298.9	296.7	294.6	292.3	291.1	290.2	289.3	287.9	286.7	286.0	284.9
*Ln*2–O3	239.4	237.9	234.7	233.4	230.0	227.5	228.2	226.0	221.8	221.9	220.7
*Ln*2–O4	239.4	238.6	235.7	231.6	230.3	227.6	227.1	225.8	224.2	222.6	222.6
*Ln*2–O7	239.9	238.0	233.1	232.6	230.2	229.4	228.0	226.6	226.8	225.4	224.4
*Ln*2–O1	239.5	239.0	234.4	233.3	230.7	228.9	228.8	227.8	226.7	224.7	223.6
*Ln*2–O5	240.3	239.5	237.1	235.0	232.1	232.5	229.3	228.6	226.2	225.6	224.5
*Ln*2–O8	257.2	255.0	251.1	249.0	245.8	242.6	241.7	239.0	238.5	234.5	234.6
*Ln*2–O6	283.5	282.7	282.6	282.8	*292.7*	*296.3*	*304.1*	*314.0*	*325.2*	*331.7*	*335.2*
*Ln*2–Br2	303.5	302.2	300.5	299.2	297.8	297.0	296.0	295.2	295.4	294.8	294.9
Mo1–O1	173.8	173.7	175.1	173.8	173.9	174.7	173.6	173.4	173.5	173.8	174.5
Mo1–O2	173.4	175.2	172.4	174.3	173.5	173.1	173.5	173.7	176.2	173.2	173.7
Mo1–O3	179.9	178.8	179.0	177.6	179.0	180.5	177.9	177.5	178.8	177.1	175.5
Mo1–O4	179.0	178.1	177.6	178.9	178.6	180.6	180.1	179.7	181.3	182.3	181.5
Mo2–O5	173.8	173.3	173.0	173.0	174.0	172.4	174.1	173.6	174.2	173.4	173.8
Mo2–O6	177.6	176.7	177.4	176.2	176.1	176.2	174.9	175.0	174.9	175.3	175.2
Mo2–O7	174.6	174.9	176.6	174.9	175.3	175.1	175.4	176.0	175.6	175.6	176.1
Mo2–O8	180.1	178.9	181.0	181.4	180.6	182.5	181.8	181.3	182.1	183.3	182.2
O1–Mo1–O7	110.0	109.3	109.7	109.5	109.5	109.6	109.9	109.7	109.5	109.6	109.8
O1–Mo1–O3	112.7	112.8	113.5	112.7	113.0	112.2	112.7	111.8	111.0	111.2	101.1
O1–Mo1–O4	110.1	110.6	110.6	111.0	110.6	111.0	110.3	110.9	111.4	111.5	111.5
O2–Mo1–O3	111.8	111.8	111.1	112.0	112.0	112.8	112.2	112.1	111.1	110.9	110.2
O2–Mo1–O4	112.5	112.6	112.5	111.9	112.4	112.4	112.2	112.0	112.0	111.8	111.4
O3–Mo1–O4	99.3	99.5	99.1	99.4	99.1	98.6	99.2	100.2	101.7	101.7	103.8
O5–Mo2–O6	111.7	111.7	111.7	111.6	111.0	110.9	109.7	109.7	109.0	108.7	108.7
O5–Mo2–O7	108.5	108.6	108.4	108.2	108.1	108.2	107.7	107.9	107.2	106.6	106.6
O5–Mo2–O8	112.6	112.8	112.7	112.9	112.8	112.8	112.7	112.0	111.9	111.9	111.6
O6–Mo2–O7	112.4	112.1	112.7	112.0	111.5	111.0	111.8	110.3	110.3	110.0	109.9
O6–Mo2–O8	99.8	99.8	99.5	99.6	100.8	100.6	101.8	102.7	104.0	103.9	104.7
O7–Mo2–O8	111.8	111.7	112.3	112.6	112.7	113.2	113.7	114.1	114.3	115.6	115.3

X-Ray structure determinations

Intensity data sets for all single crystals of the LnBr[MoO_4] series (Ln = Pr, Nd, Sm, Gd – Lu) were collected on a Nonius Kappa-CCD diffractometer using graphite-monochromatized MoK_α radiation (wavelength: $\lambda = 71.07$ pm). A numerical absorption correction was performed with the program HABITUS [7] in all cases. The structure solutions and refinements were carried out utilizing the program package SHELX-97 [8]. Details of the data collections and structure refinements [9] are summarized in Table 1, interatomic distances can be found in Table 2 and the motifs of mutual adjunction [10 – 13] in Table 3.

Further details of the crystal structure investigation may be obtained from Fachinformationszentrum Karlsruhe, 76344 Eggenstein-Leopoldshafen, Germany (fax: +49-7247-808-666; e-mail: crysdata@fiz-karlsruhe.de, http://www.fiz-karlsruhe.de/request_for_deposited_data.html) on quoting the deposition numbers CSD-425263 for PrBr[MoO_4], CSD-425264 for NdBr[MoO_4], CSD-425265 for SmBr[MoO_4], CSD-425266 for GdBr[MoO_4], CSD-425267 for TbBr[MoO_4], CSD-425268 for DyBr[MoO_4], CSD-425269 for HoBr[MoO_4], CSD-425270 for ErBr[MoO_4], CSD-425271 for TmBr[MoO_4], CSD-425272 for YbBr[MoO_4], and CSD-425273 for LuBr[MoO_4].

Results and Discussion

The lanthanoid(III) bromide ortho-oxomolybdates(VI) with the formula LnBr[MoO_4] (Ln = Pr, Nd, Sm, Gd – Lu) crystallize isotypically with

Table 3. Motifs of mutual adjunction [10 – 13] for the triclinic LnBr[MoO_4] series for Ln = Pr, Nd, Sm, Gd (top), Ln = Tb, Dy, Ho, Er (mid), Ln = Tm, Yb, Lu (bottom).

	*Ln*1	*Ln*2	Mo1	Mo2	CN
Br1	2 / 2	0 / 0	0 / 0	0 / 0	2
Br2	1/ 1	1 / 1	0 / 0	0 / 0	2
O1	0 / 0	1 / 1	1 / 1	0 / 0	2
O2	1/ 1	0 / 0	1 / 1	0 / 0	2
O3	1/ 1	1 / 1	1 / 1	0 / 0	3
O4	1/ 1	1 / 1	1 / 1	0 / 0	3
O5	0 / 0	1 / 1	0 / 0	1 / 1	2
O6	1 / 1	1 / 1	0 / 0	1 / 1	2
O7	0 / 0	1 / 1	0 / 0	1 / 1	2
O8	1 / 1	1 / 1	0 / 0	1 / 1	3
CN	8	8	4	4	
	*Ln*1	*Ln*2	Mo1	Mo2	CN
Br1	2 / 2	0 / 0	0 / 0	0 / 0	2
Br2	1/ 1	1 / 1	0 / 0	0 / 0	2
O1	0 / 0	1 / 1	1 / 1	0 / 0	2
O2	1/ 1	0 / 0	1 / 1	0 / 0	2
O3	1/ 1	1 / 1	1 / 1	0 / 0	3
O4	1/ 1	1 / 1	1 / 1	0 / 0	3
O5	0 / 0	1 / 1	0 / 0	1 / 1	2
O6	1 / 1	0 / 0	0 / 0	1 / 1	2
O7	0 / 0	1 / 1	0 / 0	1 / 1	2
O8	1 / 1	1 / 1	0 / 0	1 / 1	3
CN	8	7	4	4	
	*Ln*1	*Ln*2	Mo1	Mo2	CN
Br1	2 / 2	0 / 0	0 / 0	0 / 0	2
Br2	1/ 1	1 / 1	0 / 0	0 / 0	2
O1	0 / 0	1 / 1	1 / 1	0 / 0	2
O2	1/ 1	0 / 0	1 / 1	0 / 0	2
O3	0 / 0	1 / 1	1 / 1	0 / 0	3
O4	1/ 1	1 / 1	1 / 1	0 / 0	3
O5	0 / 0	1 / 1	0 / 0	1 / 1	2
O6	1 / 1	0 / 0	0 / 0	1 / 1	2
O7	0 / 0	1 / 1	0 / 0	1 / 1	2
O8	1 / 1	1 / 1	0 / 0	1 / 1	3
CN	7	7	4	4	

$YBr[MoO_4]$ [14] in the triclinic system (space group: $P\bar{1}$ (no. 2); $a = 686 - 689$, $b = 713 - 741$, $c = 1066 - 1121$ pm, $\alpha = 103 - 106$, $\beta = 107 - 108$, $\gamma = 92 - 95°$; $Z = 4$, see Table 1). The crystal structures contain two crystallographically different lanthanoid(III) cations, which both exhibit a coordination number of 7 + 1. $(Ln1)^{3+}$ is surrounded by three bromide and four *plus* one oxide anions in the shape of a trigonal dodecahedron (Fig. 1, top left). The coordination sphere around $(Ln2)^{3+}$ consists of six oxide anions which form a trigonal prism. The rectangular faces of this prism are capped by one bromide anion and, for the larger lanthanoid(III) cations, an additional oxide anion acts as another cap (Fig. 2, top right). The interatomic distances from the central lanthanoid

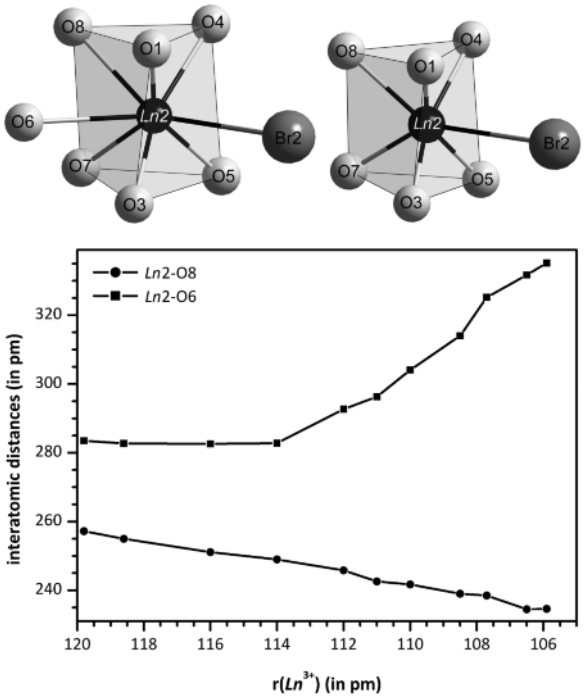

Fig. 2. Coordination polyhedra around the $(Ln2)^{3+}$ cations (Ln = Pr, Nd, Sm, Gd, top left; Ln = Tb – Lu, top right) and a graphical display of the second longest (Ln2–O6) and longest Ln–O distances (Ln2–O8) in the crystal structure of the LnBr[MoO_4] representatives with Ln = Pr, Nd, Sm and Gd – Lu (bottom).

cations to their oxide ligands range between 238 and 264 pm for PrBr[MoO_4], with Pr^{3+} being the largest Ln^{3+} cation in the presented series, and between 214 and 229 pm for LuBr[MoO_4], with Lu^{3+} as the smallest one. These values are in good agreement with those found in Pr_2O_3 (d(Pr–O) = 231 – 268 pm) [15] and PrOBr (d(Pr–O) = 235 pm) [16] as well as in Lu_2O_3 (d(Lu–O) = 219 – 229 pm) [17] and $LuMnO_3$ (d(Lu–O) = 218 – 242 pm) [18]. For PrBr[MoO_4] an additional Pr^{3+}–O^{2-} contact of 284 pm (Pr1–O6) can also be identified, which provides a small, but not negligible, contribution to the *E*ffective *Co*ordination *N*umber (ECoN, according to Hoppe [19]) of Pr^{3+}. The decrease in the size of the Ln^{3+} cation throughout the presented series results in a small decrease within the range of the aforementioned longer distances between $(Ln2)^{3+}$ and O^{2-} to the point of a limit of the ionic radius of $(Ln2)^{3+}$, observed at the element terbium, where a strong increase of the $(Ln2)^{3+}$–O^{2-} distance becomes immanent, so that $(O6)^{2-}$ no longer

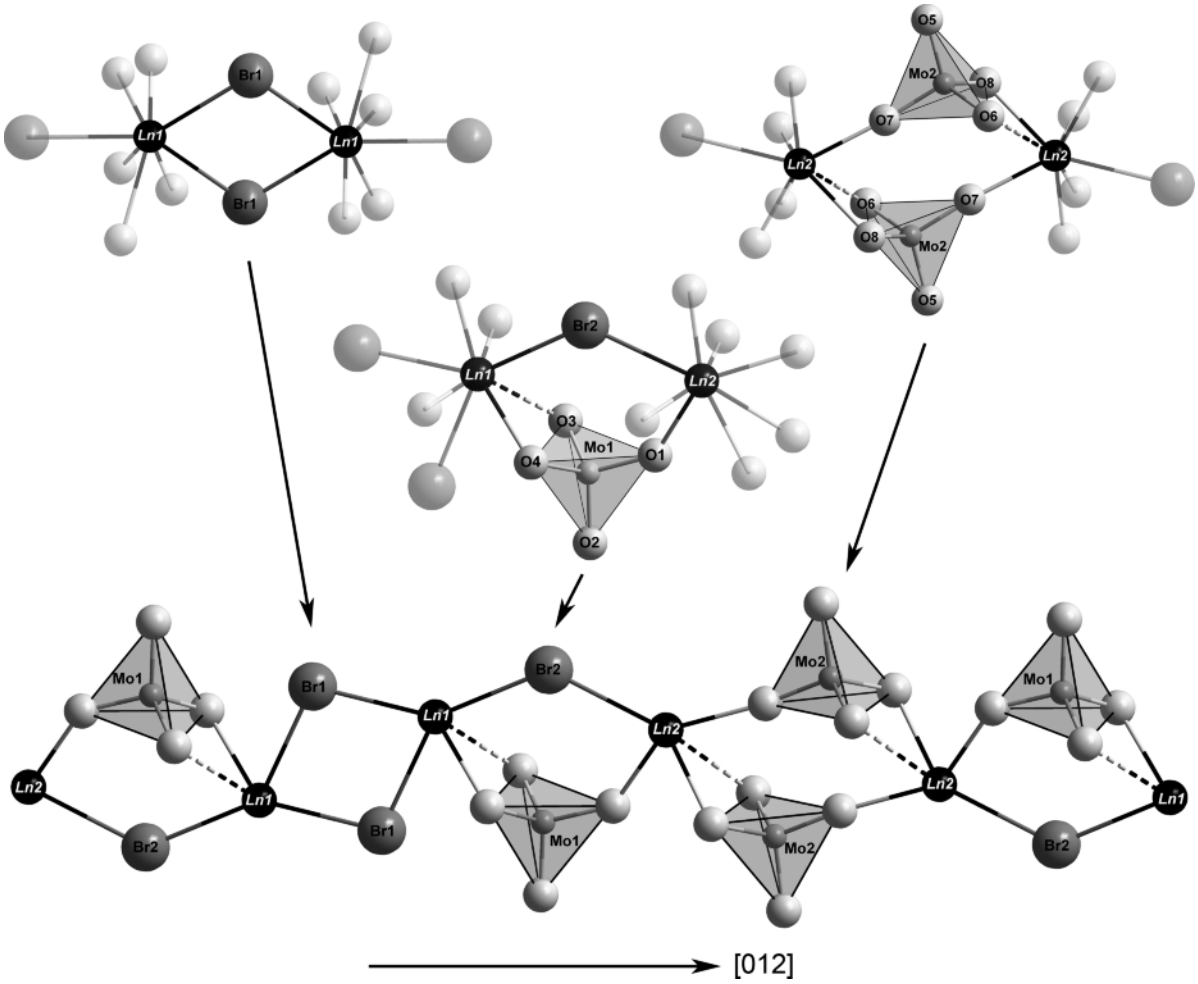

Fig. 3. Connectivity of two polyhedra around $(Ln1)^{3+}$ (top left), of two polyhedra around $(Ln2)^{3+}$ (top right), interconnection of the $(Ln1)^{3+}$- and $(Ln2)^{3+}$-centered polyhedra (mid), and the resulting chain $^{1}_{\infty}\{LnBr[MoO_4]\}$ running along [012] (bottom) in the crystal structure of the $LnBr[MoO_4]$ representatives with Ln = Pr, Nd, Sm and Gd – Lu.

provides a contribution to the respective $(Ln2)^{3+}$ coordination sphere and only monocapped trigonal $[(Ln2)O_6Br]^{10-}$ prisms result as coordination polyhedra (Fig. 2, top right). The same is true for the $(O3)^{2-}$ surrounding of $(Ln1)^{3+}$ (Fig. 1, bottom) with the radius limit at the element thulium, leaving trigonal dodecahedra $[(Ln1)O_{4+1}Br_3]^{10-}$ with one oxygen atom (O3) stripped off (Fig. 1, top right). The distances between $Pr^{3+}$and Br^- in $PrBr[MoO_4]$ range between 298 and 304 pm, correspond very well with those in ternary K_2PrBr_5 (d(Pr–Br) = 292 – 303 pm) [20] and rather fair with those in binary $PrBr_3$ (d(Pr–Br) = 309 – 315 pm) [21]. In the area of compounds comprising both Lu^{3+} and Br^- ions, only few examples are known in the literature, and none of these display the wide range of Lu^{3+}–Br^- distances (284 – 304 pm) as found in $LuBr[MoO_4]$. However, since the structures of LuSBr (d(Lu–Br) = 278 pm) [22] and LuOBr (d(Lu–Br) = 312 pm) [23] are well established, the respective values of lutetium bromide oxomolybdate can be placed right in between these other two ternary lutetium-bromide compounds.

The structure of the $LnBr[MoO_4]$ representatives consists of two different tetrahedral ortho-oxomolybdate(VI) units $[MoO_4]^{2-}$, which are surrounded by five Ln^{3+} cations each *via* sharing

edges and corners. The Mo^{6+}–O^{2-} bond lengths display values of 172 – 183 pm, which are in accord with those found in the *Ln*Cl[MoO_4] series (d(Mo–O) = 172 – 179 pm) [6] or in scheelite-type Ba[MoO_4] (d(Mo–O) = 185 pm) [24]. The deviation of the O–Mo–O angles from the typical tetrahedral one of 109.5° is about 10 %. The angles in the $[MoO_4]^{2-}$ tetrahedra of the title compounds thus cover the interval from 99 to 116°. Both crystallographically different bromide anions exhibit coordination numbers of two and are coordinated in an angular fashion (*Ln*1–Br1–*Ln*1: 105.7 – 106.4°, *Ln*1–Br2–*Ln*2: 131.7 – 134.0°). The structural motif of the *Ln*Br[MoO_4] representatives is easily described by the interconnection of the coordination polyhedra of the Ln^{3+} cations. Those

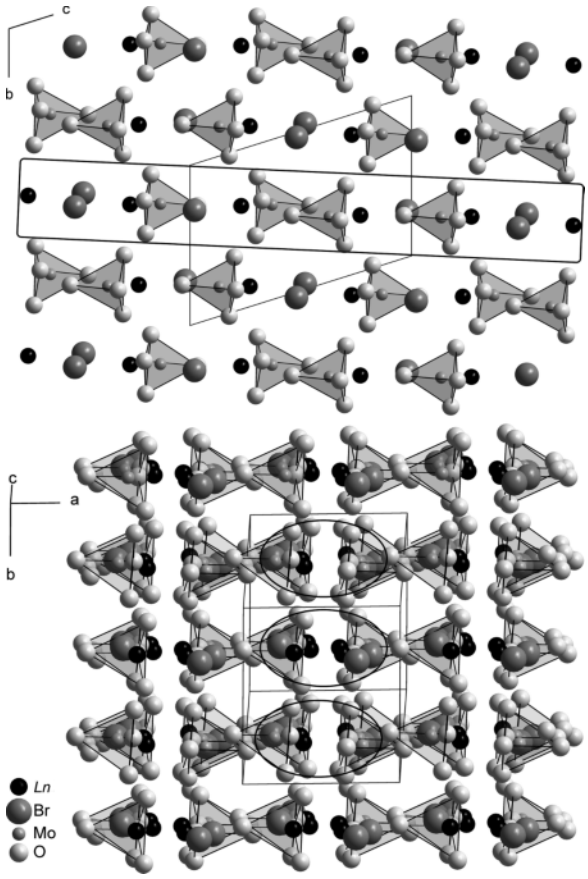

Fig. 4. View at the crystal structure of the *Ln*Br[MoO_4] series (*Ln* = Pr, Nd, Sm, Gd – Lu) along [100] (top) and along [012] (bottom) emphasizing the position of the $^1_\infty\{$*Ln*Br[MoO_4]$\}$ chains described in Fig. 3.

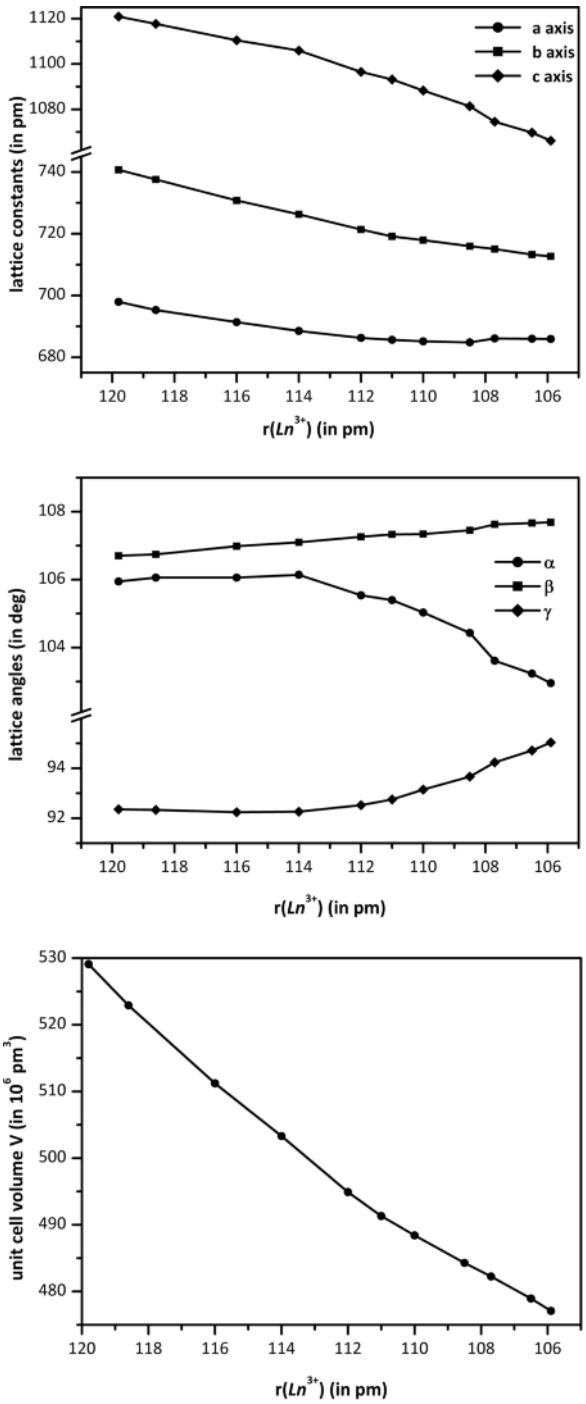

Fig. 5. Development of the lattice constants a, b, c (top), the lattice angles α, β, γ (mid), and the unit cell volumes V (bottom) in the *Ln*Br[MoO_4] series (*Ln* = Pr, Nd, Sm, Gd – Lu).

around $(Ln1)^{3+}$ are connected to each other *via* common edges, which consist of two $(Br1)^{-}$ anions (Fig. 3, top left), while the polyhedra around $(Ln2)^{3+}$ are fused together by oxide anions of two $[(Mo2)O_4]^{2-}$ tetrahedra (Fig. 3, top right). Finally, the polyhedra around $(Ln1)^{3+}$ are joined with those around $(Ln2)^{3+}$ by means of one $(Br2)^{-}$ anion and one $[(Mo1)O_4]^{2-}$ tetrahedron (Fig. 3, mid). The resulting chains according to $^{1}_{\infty}\{LnBr[MoO_4]\}$ (Fig. 3, bottom) proceed along [012] in the crystal structure of the title compounds (Fig. 4).

In the crystal structure of the lanthanoid(III) bromide ortho-oxomolybdates(VI) with the formula $LnBr[MoO_4]$ (Ln = Pr, Nd, Sm, Gd – Lu) a decrease of the lattice parameters as well as the molar volumes is observed as a result of the lanthanoid contraction (Table 1). Hence, the lattice dimensions (particularly those of the a and c axes) display a mostly linear trend with only a slight unsteadiness on passing from the Er^{3+} to the Tm^{3+} member (Fig. 5, top). The lattice angles, however, exhibit a peculiar behavior. The angle β steadily increases, thus reducing the volume of the unit cell, while α increases and γ decreases, both in a non-linear way (Fig. 5, mid). Nonetheless, in the overall contraction process a steady, almost linear reduction of the molar volume with respect to the ionic radius of the shrinking Ln^{3+} cation is observed (Fig. 5, bottom). A comparison of the title compounds with their formula-analogous chloride oxomolybdates(VI) $LnCl[MoO_4]$ reveals differences in both the structural setup and the coordination behavior of the involved Ln^{3+} cations. While in the $LnCl[MoO_4]$ representatives with Ln = Nd [25] and Sm – Lu [6] three different structure types can be distinguished, in which the polyhedra around the Ln^{3+} cations are condensed to form a three- (Ln = Nd [25]), two- (Ln = Sm – Yb [6]), or one-dimensional arrangement (Ln = Lu [6]), the fundamental architecture of the bromide homologs remains unchanged throughout the whole series presented here. The details, however, also reflect the course of the contracting coordination environment of the Ln^{3+} cations. In the bromide derivatives, a gradual detachment of a single oxide anion from the central lanthanoid(III) cations can be detected by passing through the series from the praseodymium to the lutetium compound, which yet leaves the general structure basically intact. The coordination number for Ln^{3+} in the similar chloride homologs changes abruptly from eight to seven between the $LnCl[MoO_4]$ representatives with Ln = Nd [25], Sm – Yb [6] and $LuCl[MoO_4]$ [6], but for the structural change between $NdCl[MoO_4]$ and the other compounds in the chloride-derivative series there is no obvious explanation.

Conclusion

In this article the syntheses and crystal structures of the bromide-derivatized lanthanoid(III) ortho-oxomolybdates(VI) $LnBr[MoO_4]$ are described for Ln = Pr, Nd, Sm and Gd – Lu. Furthermore, the similarities and differences to the non-isotypic structures of the homologous series $LnCl[MoO_4]$ (Ln = Pr [4], Nd [25], Sm – Lu [6]) and $LnF[MoO_4]$ (Ln = Sm – Tm [2]) are shown in a detailed structural comparison, which includes a special consideration of their triclinic lattice constants as a function of the lanthanoid contraction.

Acknowledgement

The authors like to thank the State of Baden-Württemberg (Stuttgart, Germany) and the Fonds der Chemischen Industrie (Frankfurt am Main, Germany) for financial support.

[1] Th. Schleid, S. Strobel, P. K. Dorhout, P. Nockemann, K. Binnemans, I. Hartenbach, *Inorg. Chem.* **2008**, *47*, 3728 – 3735.
[2] I. Hartenbach, S. Strobel, P. K. Dorhout, Th. Schleid, *J. Solid State Chem.* **2008**, *181*, 2828 – 2836.
[3] I. Hartenbach, S. Strobel, Th. Schleid, B. Sarkar, W. Kaim, P. Nockemann, K. Binnemans, P. K. Dorhout, *Eur. J. Inorg. Chem.* **2010**, *2010*, 1626 – 1632.
[4] I. Hartenbach, Th. Schleid, S. Strobel, P. K. Dorhout, *Z. Anorg. Allg. Chem.* **2010**, *636*, 1183 – 1189.
[5] I. Hartenbach, H. Henning, Th. Schleid, T. Schustereit, S. Strobel, *Z. Anorg. Allg. Chem.* **2013**, *639*, 347 – 353.
[6] I. Hartenbach, S. Strobel, Th. Schleid, K. W. Krämer, P. K. Dorhout, *Z. Anorg. Allg. Chem.* **2009**, *635*, 966 – 975.
[7] W. Herrendorf, H. Bärnighausen, HABITUS, Program for the Optimization of the Crystal Shape for Numerical Absorption Correction, Universities of Karlsruhe and Gießen, Karlsruhe, Gießen **1993**, **1996**; as implemented in X-SHAPE (version 1.06), Stoe & Cie GmbH, Darmstadt (Germany) **1999**.
[8] G. M. Sheldrick, *Acta Crystallogr.* **2008**, *A64*, 112 – 122.

[9] Th. Hahn, A. J. C. Wilson (Eds.), *International Tables for Crystallography*, Vol. C, 2nd Edit., Kluwer Academic Publishers, Boston **1992**.
[10] R. Hoppe, *Adv. Fluorine Chem.* **1970**, *6*, 387 – 438.
[11] R. Hoppe, *Izv. Jugoslav. Centr. Krist. (Zagreb)* **1973**, *8*, 21 – 36.
[12] R. Hoppe in *Crystal Structure and Chemical Bonding in Inorganic Chemistry*, (Eds.: C. J. M. Rooymans, A. Rabenau), North Holland Publ. Comp., Amsterdam **1975**, pp. 127 – 161.
[13] R. Hoppe, *Angew. Chem., Int. Ed. Engl.* **1980**, *19*, 110 – 125.
[14] H. Henning, T. Schustereit, Th. Schleid, I. Hartenbach, *Z. Kristallogr.* **2012**, *Suppl. 32*, 95 – 96.
[15] O. Greis, R. Ziel, B. Breidenstein, A. Haase, T. Petzel, *J. Alloys Compd.* **1994**, *216*, 255 – 258.
[16] P. Talmon-Gros, C. M. Schurz, Th. Schleid, *Acta Crystallogr.* **2011**, *E67*, i74.
[17] H. Bommer, *Z. Anorg. Allg. Chem.* **1939**, *241*, 273 – 280.
[18] H. L. Yakel, Jr., W. C. Köhler, E. F. Bertaut, E. F. Forrat, *Acta Crystallogr.* **1963**, *16*, 957 – 962.
[19] R. Hoppe, *Z. Kristallogr.* **1979**, *150*, 23 – 52.
[20] G. Meyer, J. Soose, A. Moritz, V. Vitt, Th. Holljes, *Z. Anorg. Allg. Chem.* **1985**, *521*, 161 – 172.
[21] W. H. Zachariasen, *Acta Crystallogr.* **1948**, *1*, 265 – 268.
[22] G. Collin, C. Dagron, F. Thévet, *Bull. Soc. Chim. Franç.* **1974**, 418 – 420.
[23] S. Zimmermann, I. Pantenburg, G. Meyer, *Acta Crystallogr.* **2007**, *E63*, i156.
[24] V. Nassif, R. E. Carbonio, J. A. Alonso, *J. Solid State Chem.* **1999**, *146*, 266 – 270.
[25] I. Hartenbach, Th. Schleid, *Z. Anorg. Allg. Chem.* **2009**, *635*, 1904 – 1909.